

BLUETOOTH LOW ENERGY AND CNN-BASED ANGLE OF ARRIVAL LOCALIZATION IN PRESENCE OF RAYLEIGH FADING

Zohreh HajiAkhondi-Meybodi[†], Mohammad Salimibeni[‡], Arash Mohammadi[‡], Konstantinos N. Plataniotis^{††}

[†] Electrical and Computer Engineering, Concordia University, Montreal, Canada

[‡] Concordia Institute of Information Systems Engineering (CIISE), Montreal, Canada

^{††} Electrical and Computer Engineering, University of Toronto, Toronto, Canada

ABSTRACT

Bluetooth Low Energy (BLE) is one of the key technologies empowering the Internet of Things (IoT) for indoor positioning. In this regard, Angle of Arrival (AoA) localization is one of the most reliable techniques because of its low estimation error. BLE-based AoA localization, however, is in its infancy as only recently direction-finding feature is introduced to the BLE specification. Furthermore, AoA-based approaches are prone to noise, multi-path, and path-loss effects. The paper proposes an efficient Convolutional Neural Network (CNN)-based indoor localization framework to tackle these issues specific to BLE-based settings. We consider indoor environments without presence of Line of Sight (LoS) links affected by Additive White Gaussian Noise (AWGN) with different Signal to Noise Ratios (SNRs) and Rayleigh fading channel. Moreover, by assuming a 3-D indoor environment, the destructive effect of the elevation angle of the incident signal is considered on the position estimation. The effectiveness of the proposed CNN-AoA framework is evaluated via an experimental testbed, where In-phase/Quadrature (I/Q) samples, modulated by Gaussian Frequency Shift Keying (GFSK), are collected by four BLE beacons. Simulation results corroborate effectiveness of the proposed CNN-based AoA technique to track mobile agents with high accuracy in the presence of noise and Rayleigh fading channel.

Index Terms— Angle of Arrival (AoA), Bluetooth Low Energy (BLE), Convolutional Neural Network (CNN), Indoor Localization, Internet of Things (IoT).

1. INTRODUCTION

Bluetooth Low Energy (BLE), as one of the most reliable and low power consuming Radio Frequency (RF) technologies, offers the ability to continuously monitor mobile users in indoor environments. Given its unique characteristics, BLE has been widely utilized in different Internet of Things (IoT) applications for localization and positioning tasks [1]. Existing BLE-based indoor localization solutions are, typically, developed based on trilateration [2, 3], triangulation [4, 5], fingerprinting [6], and/or Pedestrian Dead Reckoning (PDR) [7] techniques. One of the most efficient triangulation methods to measure the location of mobile devices is to calculate the Angle of Arrival (AoA). BLE-based AoA estimation, however, was not possible until recently that direction finding feature is introduced to the Bluetooth 5.1 Core specification. Consequently, research works in this area is still in its infancy. The paper aims to further advance this emerging field.

Literature Review: AoA-based localization, as an active research field for several decades, is a nonlinear triangulation approach to measure the position of mobile agents based on the direction of the incident radio frequency signal, received by an antenna array such

as Linear Antenna Array (LAA) [8, 14]. Subspace-based angle estimation algorithms [15, 16], such as Multiple Signal Classification (MUSIC) and its extensions, are among the early research efforts for AoA estimation. Despite the benefits that can be obtained by using subspace-based angle estimation techniques, such localization methods suffer from some drawbacks. A key limitation is the unreliability of the subspace-based algorithms in the presence of the multi-path effect, which is an unavoidable factor in indoor environments [17]. Multi-path fading channel in indoor environments is commonly modeled by statistical models mainly Rayleigh [18, 19] and Rician [20]. By assuming that there is a strong Line of Sight (LoS) path between the transmitter and the receiver, there are a wide range of approaches to address the multi-path propagation, including channel classification [21], Kalman filter-based techniques [22], and subsample interpolation methods [23]. Presence of different objects within indoor environments, however, leads to receiving the reflected, refracted, diffracted, and scattered versions of the transmitted wireless signal. Consequently, the assumption of existing a strong LoS path is not practical in most indoor localization scenarios. The most important novelty of this paper is that we consider the worst-case scenario, i.e., a dense indoor environment that it is not possible to establish LoS link. On the other hand, due to the complexity of analytical modelling of the multi-path and path-loss effects in indoor environments, the focus has shifted to data-driven approaches such as those based on Deep Neural Networks (DNNs) [24]. Therefore, by considering the effects of multi-path and path-loss on the train dataset, one can eliminate the need for complex and precise analytical models. Capitalizing on these advantages, we focus on the data AoA estimation with the emphasis on the Convolutional Neural Networks (CNNs). In this regard, for instance Reference [25] introduced a CNN-based localization approach for the 2-D AoA estimation in the presence of noise. Authors in [26] investigated the effect of noise in a 3-D environment on the angle estimated by employing DNNs. Authors in [27, 28] proposed a DNN-based localization framework, where the input of the DNN is the Channel Impulse Response (CSI)-AoA images. CSI, however, is prone to the noise, shadowing, and small scale fading, leading to a considerable localization error. For this reason, we consider angle images as the input of the CNN, where angle images are constructed based on the 3-D subspace-based method, which is robust against noise.

Contributions: Although AoA estimation is one of the most reliable localization techniques, research on data driven BLE-based AoA localization is very limited [26] as only recently direction-finding feature is introduced to the BLE specification. In particular, the challenge of modeling the wireless channel as a combination of Rayleigh fading and noise without presence of the LoS link between the transmitter and the receiver in a 3-D indoor environment has not

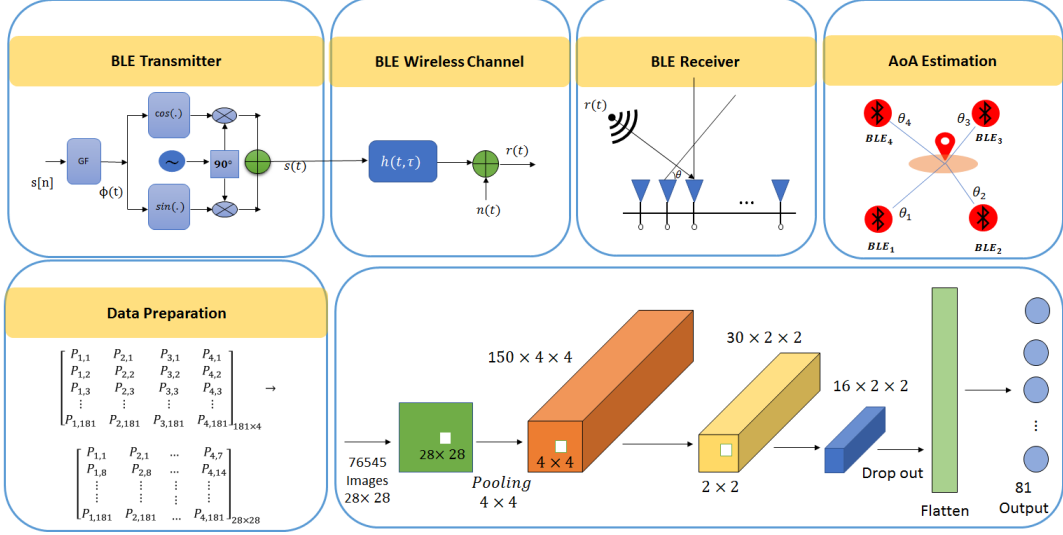


Fig. 1. Block diagram of the BLE transceiver, wireless channel model, and the proposed CNN-based AoA localization framework.

yet been considered. The paper addresses this gap. In this regard, the paper proposes an efficient CNN-based AoA localization framework for BLE-based indoor tracking within an indoor environment affected by Additive White Gaussian Noise (AWGN) with different Signal to Noise Ratios (SNRs) and Rayleigh fading channel. In such real indoor environments, mobile agents and BLE beacons are not always located along the same line, which in turn leads to elevation angle. Although the azimuth angle of the incident signal is utilized for location estimation, the destructive effect of elevation angle should be considered. Therefore, we generate AoA measurements in a 3-D indoor environment based on the subspace-based angle estimation framework. The raw AoA measurement data, which is obtained in the previous phase, is directly used by the CNN. The input of the CNN architecture is an angle image, where each pixel indicates the spatial spectrum of the AoA measurement.

The rest of the paper is organized as follows: In Section 2, the BLE wireless signal model is described. Section 3 presents the proposed CNN-based AoA localization framework. Section 4 presents experimental results. Finally, Section 5 concludes the paper.

2. BLE WIRELESS SIGNAL MODEL

The overall structure of the proposed CNN-based AoA framework is depicted in Fig. 1. In order to calculate the angle of the incident signal, first, a Gaussian Frequency Shift Keying (GFSK) transceiver, including the transmitter, the wireless channel model, and the receiver in the BLE standard, is formulated below.

2.1. BLE Transmitter

BLE has played a crucial role in the development of IoT applications because of its robustness, low-power consumption and cost efficient. BLE technology, like Wireless LAN and IEEE 802.15.4/Zig-Bee uses the same spectrum of Industrial, Scientific, and Medical (ISM) band in 2.4 to 2.48 GHz frequency range, which is divided into 40 channels with 2 MHz bandwidth. To decrease the interference from other technologies in the sharing ISM band, BLE employs Frequency Hopping (FH) method, to jump on the carrier frequency across all data channels. Among all 40 available channels, supported by BLEs, there are 37 data channels for data transmission and 3 advertisement channels [29]. After connection initialization, BLE devices transmit data packets over 37 data channels, where i^{th} packet is sent over $f_i = f_{i-1} + f_{hop} \bmod 37$ BLE's channel. Note that f_{hop} is the frequency hop value to diminish the interference within BLE

channels. The baseband version of the transmitted signal, denoted by $s_b(t)$, is expressed as

$$\begin{aligned} s_b(t) &= s_i^b(t) + j s_q^b(t) \\ &= \sqrt{\frac{2E}{T}} \left\{ \cos(\phi(t) + \phi_0) + j \sin(\phi(t) + \phi_0) \right\}. \end{aligned} \quad (1)$$

By considering the fact that the GFSK modulation only affects the phase of the signal, E and T , denoting the energy and period of the transmitted symbol, are constant. ϕ_0 illustrates the initial phase of the incident signal, and $\phi(t)$ is expressed as follows

$$\phi(t) = \frac{\pi \iota}{T} \int_{-\infty}^t \sum_{n=-\infty}^{+\infty} s[n] g(\tau - nT) d\tau, \quad (2)$$

where ι , known as the modulation index, is between 0.45 to 0.55 in the BLE standard. $s[n] = \pm 1$ denotes the baseband pulse sequence. $g[k]$ as the Gaussian Filter (GF), implemented in discrete-time domain with a sample period of T_s , is obtained as

$$g(t) = \frac{\iota T_s}{2\sigma\sqrt{2\pi}} e^{-\frac{t^2}{2\sigma^2}} \otimes \text{rect}(T, t), \quad (3)$$

where \otimes is the convolution operator. Term σ is equal to $0.13T/(BT)$, where B , known as the GF 3 dB bandwidth, is equivalent to 0.5 in the BLE standard. Moreover, $\text{rect}(T, t)$ is obtained as

$$\text{rect}(T, t) = \begin{cases} \frac{1}{T}, & -\frac{T}{2} \leq t \leq \frac{T}{2} \\ 0, & \text{otherwise} \end{cases}. \quad (4)$$

Considering that the transmitted signal is $s(t) = \text{Re}\{s_b(t)e^{j2\pi f_c t}\}$, we have

$$s(t) = \sqrt{\frac{2E}{T}} \cos(2\pi f_c t + \phi(t) + \phi_0), \quad (5)$$

where $2.4 \leq f_c \leq 2.48$ GHz denotes the carrier frequency.

2.2. BLE Channel Model

In an indoor environment, $N(t)$ number of phase delayed and power attenuated versions of the transmitted signal $s(t)$ are provided in the receiver side, which is known as the wireless multipath fading

channel. In addition, by traveling a distance, the transmitted signal becomes weaker as a result of the path loss effect. The baseband channel impulse response, denoted by $h_b(t, \tau)$, as a Complex Finite Impulse Response (FIR) filter illustrates both multi-path and path loss effects on the transmitted signal as follows

$$h_b(t, \tau) = \sum_{k=1}^{N(t)} \rho_k(t, \tau) e^{-j\theta_k(t)} \delta(t - \tau_k(t)), \quad (6)$$

where $\tau_k(t)$, $\theta_k(t) = 2\pi f_c \tau_k(t)$, and $\rho_k(t, \tau)$ denote the k^{th} path delay, phase shift, and path attenuation, respectively.

2.3. BLE Receiver

AoA measurement can be performed by determining the direction of the propagation signal on an antenna array, including two or more antennas. For this reason, it is assumed that all the BLE beacons possess a LAA (see Fig. 1). The continuous-time signal $r(t)$, which is a distorted version of the transmitted signal, is received by each element with a phase difference. In addition to the wireless multipath fading channel, noise has a destructive impact on the transmitted signal, as well. Considering all these aspects to define $r_b(t)$ as the baseband received signal, we have

$$r_b(t) = (s_b(t) * h_b(t, \tau)) \frac{1}{2} e^{j2\pi f_e(t)t + \varphi_e(t)} + n(t), \quad (7)$$

where $\varphi_e(t)$ and $f_e(t)$ denote the phase and frequency shifts, respectively. Note that the frequency shift happens because of the transmitter's carrier frequency asynchronicity. Based on the narrowband assumption, the frequency response can be considered flat, which means the delay spread is small compared to the symbol duration. Therefore, we have $s(t - \tau_k(t)) \simeq s(t)$ [29]. Consequently, the received signal $r(t)$ by a BLE beacon is expressed as follows

$$r(t) = \alpha(t)s(t) + n(t) = s'(t) + n(t), \quad (8)$$

where $n(t) \sim \mathcal{N}(0, \sigma^2)$ denotes the AWGN, and $\alpha(t)$, as the channel model, is obtained based on Eqs. (6) and (7) as follows

$$\alpha(t) = \sum_{k=1}^{N(t)} \rho_k(t, \tau) e^{-j\theta_k(t) + j2\pi f_c t + \varphi_c(t)}. \quad (9)$$

This completes presentation of the BLE wireless signal model. Next, we present the proposed CNN-based AoA localization framework.

3. THE CNN-BASED AOA LOCALIZATION FRAMEWORK

The proposed CNN-based AoA framework is performed in two phases, i.e., AoA measurement in a 3-D indoor environment, and location estimation based on the CNN algorithm, described below.

3.1. AoA measurement in a 3-D Indoor Environment

We consider a subspace-based angle estimation in a 3-D environment, where the incident signal has both azimuth θ and elevation ϕ angles. There are N_e elements in the LAA, receiving the same signal with different phases. By assuming $\lambda = \frac{c}{f_c}$, where $c = 3 \times 10^8$ m/s is the speed of light, the discrete received signal by element e , which is sampled at the discrete time slot m , denoted by $r_e[m]$, is obtained as follows

$$r_e[m] = s'[m]\Theta(\theta, \phi)[m] + n[m], \quad (10)$$

where $\Theta(\theta, \phi)$ denotes the array vector, defined as follows

$$\Theta(\theta, \phi) = \begin{bmatrix} \exp(-j\frac{2\pi d}{\lambda} \cos \theta \cos \phi), \\ \exp(-j\frac{2\pi d}{\lambda} \sin \theta \cos \phi), \exp(-j\frac{2\pi d}{\lambda} \sin \phi) \end{bmatrix}^T, \quad (11)$$

where d indicates the space between two consecutive elements of the LAA, which is equal to $\frac{\lambda}{2}$. By assuming M samples in each received signal, we have

$$\mathbf{r} = [r_1[m] \dots r_{N_e}[m]]^T, \quad (12)$$

$$\text{and } \mathbf{s}' = [s'_1[m] \dots s'_{N_e}[m]]^T. \quad (13)$$

Therefore, we can express the received signal in a compact form as

$$\mathbf{r} = \Theta \mathbf{s}' + \mathbf{n}. \quad (14)$$

The spatial spectrum function, denoted by $P(\theta, \phi)$, is defined as

$$\mathbf{P}(\theta, \phi) = \frac{1}{\Theta^H(\theta, \phi) \mathbf{E}_N \Theta^H(\theta, \phi)}, \quad (15)$$

where \mathbf{E}_N indicates the noise eigenvectors of the covariance matrix $\mathbf{R} = E[\mathbf{r}, \mathbf{r}^H]$. Consequently, the minimum peak of $\mathbf{P}(\theta, \phi)$ illustrates the direction of the incident signal. Given the angle of the signal from at least two BLE beacons with known positions, the location of the mobile agent can be calculated. The coordinate of the BLE beacon b is denoted by (x_b, y_b) , and $\theta_{b,n}$ indicates the angle between x -axis and the line between the BLE beacon and the mobile agent. Then, the estimated location of the mobile agent, denoted by $\hat{\mathbf{L}}_n(t) = (x_n, y_n)$, can be estimated as

$$x_n = \frac{d_{k,l} \tan \theta_{l,n}}{\tan \theta_{l,n} - \tan \theta_{k,n}}, \quad (16)$$

$$\text{and } y_n = \frac{d_{k,l} \tan \theta_{k,n} \tan \theta_{l,n}}{\tan \theta_{l,n} - \tan \theta_{k,n}}, \quad (17)$$

where $d_{k,l}$ is the distance between the l^{th} and k^{th} BLE beacons.

3.2. CNN-based Location Estimation

Given the angle of the incident signal, a data-driven approach, which is a combination of a CNN architecture and a subspace-based angle estimation algorithm, is designed to track mobile agents during their movements. The proposed architecture, as shown in Fig. 1, consists of a series of convolutional layers, pooling layers, fully connected layers, and normalization layers. Each convolutional layer, which applies a convolution operation to the input to extract spatial features, is followed by a pooling layer to down-sample the data to reduce the spatial dimension and the computation time. In each time slot/location, an angle image is provided as the input to the CNN, which is generated by feature matrices constructed based on Eq. (15), i.e., $\mathbf{P}(\theta, \phi, t) = [\mathbf{P}_1(\theta, \phi, t), \dots, \mathbf{P}_4(\theta, \phi, t)]$. Term $\mathbf{P}_i(\theta, \phi, t)$, for $(i \in \{1, \dots, 4\})$ indicates the spatial spectrum of the received signal by the i^{th} BLE beacon. This spatial spectrum is reshaped to be an square angle image (see Fig. 1). Each angle image is then labeled by the respective ground truth position $\mathbf{L}_n(t) = (x_n, y_n)$. By considering the fact that the angle of the incident signal θ could be valued between 0° and 180° , there are 181 samples in $\mathbf{P}_i(\theta, \phi, t)$, where $\mathbf{P}_i(\theta, \phi, t)$ peak in the corresponding θ . Due to the effects of noise, multi-path, and elevation angle, however, the peak of the spatial spectrum is likely to mismatch the real value θ . Therefore, the goal is to use CNN as a function approximation to estimate the location of the mobile agent from the angle image captured in each time slot. The overall structure of the proposed CNN-based AoA framework is shown in Fig. 1. To train the CNN-based AoA framework, the Mean-Squared Error (MSE) is used as the loss function $\mathcal{L}(t)$ calculated as

$$\mathcal{L}(t) = \frac{1}{2} (\mathbf{L}_n(t) - \hat{\mathbf{L}}_n(t))^2, \quad (18)$$

where the estimated location of the mobile agent $\hat{\mathbf{L}}_n(t)$ is defined in Eqs. (16) and (17).

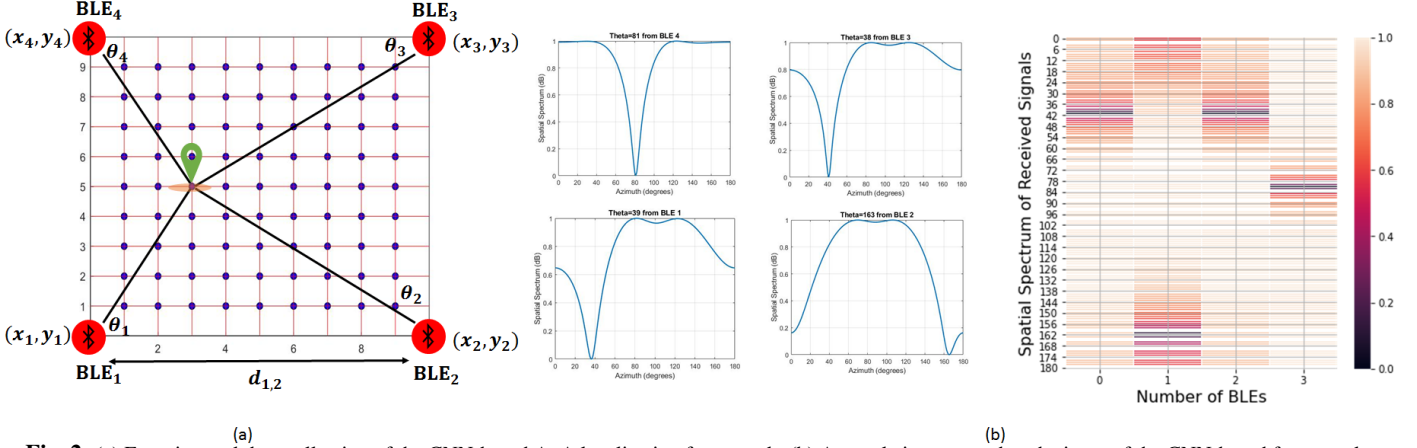


Fig. 2. (a) Experimental data collection of the CNN-based AoA localization framework. (b) An angle image, used as the input of the CNN-based framework.

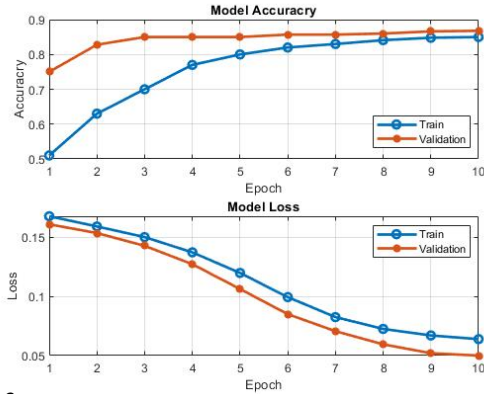


Fig. 3. Accuracy and loss of the proposed CNN-based AoA scheme.

4. SIMULATION RESULTS

To evaluate the proposed data driven and BLE-based AoA localization, we used a real experimental testbed consisting of four BLE beacons and Vicon cameras, positioned at the corner of a rectangular indoor area (5×5) m^2 to track a mobile agent and provide ground truth, respectively (see Fig. 2(a)). Without loss of generality and for simplicity, we consider a small environment [30] to generate more data for each location, and it is believed that this would not have a negative effect on the performance of the proposed algorithm from the accuracy perspective. We generated a dataset in three different channel models: (i) AWGN model, where SNR is altered between 10 dB and 20 dB; (ii) Rayleigh fading channel, implemented in MATLAB (R2020a) by the *comm.RayleighChannel* function, and; (iii) A combination of AWGN and Rayleigh fading channel in a 3-D indoor environment, divided into 81 square zones with dimension of (0.5×0.5) m^2 . Although elevation angle is not considered for location estimation, it has a destructive impact on the special spectrum of the AoA measurement, leading to a specific error in the users' tracking. For this reason, it is assumed that the incident signal is received by different elevation angles. In the training phase, 76,545 (angle image, location) training points are utilized corresponding to 81 random locations within the area. As it can be seen from Fig. 2(b), angle images contain 724 sets of AoA measurements generated by the subspace-based algorithm. This original angle image is of size 4×181 and is reshaped to be an square angle image of size 28×28 (zero padding is performed to fit the CNN model preventing data loss). In the next phase, we use 15,309 images as the validation set and 10,206 for our test set, which are all previously unseen and randomly chosen. For the CNN model, we feed our data to three 2-D convolution layers, each with 196 filters with 4 kernel size. We

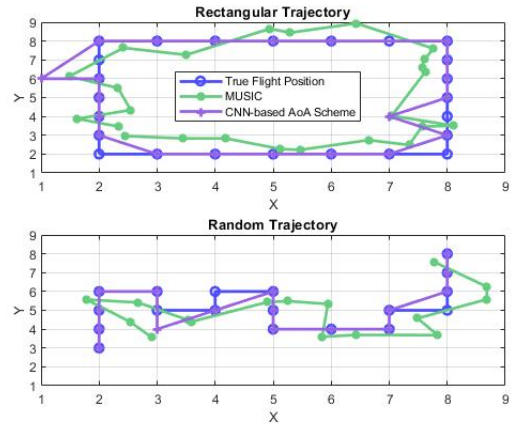


Fig. 4. Estimated rectangular and random trajectories in a 3-D indoor environment with the presence of Rayleigh fading and noise.

added maximum pooling layer and utilized sigmoid as an activation function. Finally, within the dense layers, we used linear function as the activation function.

Fig. 3 illustrates the accuracy and the loss of the proposed CNN-based AoA framework, respectively. As it can be seen from Fig. 3, increasing the number of epochs increases the model accuracy and decreases the model loss, which shows that the model is well trained. The proposed CNN-based AoA framework tracks mobile agents with 87% accuracy in the presence of noise, Rayleigh fading, and elevation angle. While the accuracy of Capon and phase difference-based frameworks are 74% and 59%, respectively. Fig. 4 compares the rectangular and random trajectories, estimated by our proposed CNN-based AoA framework, the 3-D MUSIC and the true flight position, obtained by Vicon cameras. In both scenarios, the estimated paths by the proposed CNN-based AoA framework in the most points closely follows that of the true flight positions.

5. CONCLUSION

We proposed an efficient CNN-based AoA localization framework for a 3-D indoor environment with the application to BLE standard. Although AoA estimation is one of the most reliable localization techniques, research on data driven BLE-based AoA localization is very limited given its recent introduction to the BLE specification. The paper addressed this gap. In particular, the proposed approach addresses the challenge of modeling the BLE wireless channel as a combination of Rayleigh fading and noise in a 3-D indoor environment. The experimental results illustrate that the proposed framework provides accurate results even in the presence of AWGN with different SNRs, Rayleigh fading channel, and elevation angle.

6. REFERENCES

- [1] M. Atashi, M. S. Beni, P. Malekzadeh, Z. HajiAkhondi-Meybodi, K. N. Plataniotis, and A. Mohammadi, "Orientation-Matched Multiple Modeling for RSSI-based Indoor Localization via BLE Sensors," Accepted in *28th European Signal Processing Conference (EUSIPCO)*, 2020.
- [2] B. Yang, L. Guo, R. Guo, M. Zhao, and T. Zhao, "A Novel Trilateration Algorithm for RSSI-based Indoor Localization," Accepted in *IEEE Sensors Journal*, Mar. 2020.
- [3] S. Sadowski, and P. Spachos, "RSSI-Based Indoor Localization With the Internet of Things," *IEEE Access*, vol. 6, pp. 30149-30161, June 2018.
- [4] N. H. Nguyen, and K. Dogancay, "Closed-Form Algebraic Solutions for Angle-of-Arrival Source Localization With Bayesian Priors," *IEEE Transactions on Wireless Communications*, vol. 18, no. 8, May 2019, pp. 3827-3842.
- [5] S. Monfared, T. Nguyen, L. Petrillo, P. De Doncker, and F. Horlin, "Experimental Demonstration of BLE Transmitter Positioning Based on AOA Estimation," *IEEE International Symposium on Personal, Indoor and Mobile Radio Communications (PIMRC)*, Bologna, Dec. 2018, pp. 856-859.
- [6] R. C. Luo, and T. Hsiao, "Indoor Localization System Based on Hybrid Wi-Fi/BLE and Hierarchical Topological Fingerprinting Approach," *IEEE Transactions on Vehicular Technology*, vol. 68, no. 11, pp. 10791-10806, Nov. 2019.
- [7] M. S. Beni, Z. HajiAkhondi-Meybodi, M. Atashi, P. Malekzadeh, K. N. Plataniotis, and A. Mohammadi, "IoT-TD: IoT Dataset for Multiple Model BLE-based Indoor Localization/Tracking," Accepted in *28th European Signal Processing Conference*, 2020.
- [8] P. Spachos, I. Papapanagiotou and K. N. Plataniotis, "Microlocation for Smart Buildings in the Era of the Internet of Things: A Survey of Technologies, Techniques, and Approaches," *IEEE Signal Processing Magazine*, vol. 35, no. 5, pp. 140-152, Sep. 2018.
- [9] P. Hu, Q. Bao and Z. Chen, "Target Detection and Localization Using Non-Cooperative Frequency Agile Phased Array Radar Illuminator," *IEEE Access*, vol. 7, pp. 111277-111286, Aug. 2019.
- [10] J. Zhou, H. Zhang and L. Mo, "Two-dimension localization of passive RFID tags using AOA estimation," *IEEE International Instrumentation and Measurement Technology Conference*, May 2011, pp. 1-5.
- [11] K. Wu, W. Ni, T. Su, R. P. Liu and Y. J. Guo, "Expeditious Estimation of Angle-of-Arrival for Hybrid Butler Matrix Arrays," *IEEE Transactions on Wireless Communications*, vol. 18, no. 4, pp. 2170-2185, Apr. 2019.
- [12] M. Kulin, T. Kazaz, I. Moerman, and E. De Poorter, "End-to-End Learning From Spectrum Data: A Deep Learning Approach for Wireless Signal Identification in Spectrum Monitoring Applications," *IEEE Access*, vol. 6, pp. 18484-18501, Mar. 2018.
- [13] Z. HajiAkhondi-Meybodi, M. S. Beni, K. N. Plataniotis, and A. Mohammadi, "Bluetooth Low Energy-based Angle of Arrival Estimation via Switch Antenna Array for Indoor Localization," in *Pros. International Conference on Information Fusion*, July 2020, pp. 1-6.
- [14] A. Abdallah and M. M. Mansour, "Angle-Based Multipath Estimation and Beamforming for FDD Cell-free Massive MIMO," *IEEE International Workshop on Signal Processing Advances in Wireless Communications (SPAWC)*, Cannes, France, July 2019, pp. 1-5.
- [15] L. Cheng, Y. Wu, J. Zhang and L. Liu, "Subspace Identification for DOA Estimation in Massive/Full-Dimension MIMO Systems: Bad Data Mitigation and Automatic Source Enumeration," *IEEE Transactions on Signal Processing*, vol. 63, no. 22, pp. 5897-5909, Nov. 2015.
- [16] R. Shafiq, L. Liu, J. Zhang and Y. Wu, "DoA Estimation and Capacity Analysis for 3-D Millimeter Wave Massive-MIMO/FD-MIMO OFDM Systems," *IEEE Transactions on Wireless Communications*, vol. 15, no. 10, pp. 6963-6978, Oct. 2016.
- [17] A. Yassin, Y. Nasser, M. Awad, A. Al-Dubai, R. Liu, Ch. Yuen, R. Raulefs, and E. Aboutanios, "Recent Advances in Indoor Localization: A Survey on Theoretical Approaches and Applications," *IEEE Communications Surveys & Tutorials*, vol. 19, no. 2, pp. 1327-1346, Secondquarter 2017.
- [18] J. Shen, B. Huang, X. Kang, B. Jia and W. Li, "Localization of Access Points based on the Rayleigh Lognormal Model," *IEEE Wireless Communications and Networking Conference*, 2018, pp. 1-6.
- [19] Z. P. Jiang, W. Xi, X. Li, S. Tang, J. Z. Zhao, J. S. Han, K. Zhao, Z. Wang, and B. Xiao, "Communicating is Crowdsourcing: Wi-Fi Indoor Localization with CSI-based Speed Estimation," *Journal of Computer Science and Technology*, vol. 29, no.4, pp. 589-604, 2014.
- [20] X. Wang, L. Gao and S. Mao, "BiLoc: Bi-modal Deep Learning for Indoor Localization with Commodity 5GHz WiFi," *IEEE access*, vol. 5, pp. 4209-4220, 2017.
- [21] J. He, Y. Geng, F. Liu and C. Xu, "CC-KF: Enhanced TOA Performance in Multipath and NLOS Indoor Extreme Environment," *IEEE Sensors Journal*, vol. 14, no. 11, pp. 3766-3774, Nov. 2014.
- [22] C. Zhang, X. Bao, Q. Wei, Q. Ma, Y. Yang, and Q. Wang, "A Kalman filter for UWB positioning in LOS/NLOS scenarios," in *Proc. International Conference on Ubiquitous Positioning, Indoor Navigation and Location Based Services*, Nov. 2016, pp. 73-78.
- [23] R. Exel and T. Bigler, "ToA ranging using subsample peak estimation and equalizer-based multipath reduction," in *Proc. IEEE Wireless Communications and Networking Conference (WCNC)*, Istanbul, Apr. 2014, pp. 2964-2969.
- [24] M. Z. Comiter, M. B. Crouse and H. T. Kung, "A Data-Driven Approach to Localization for High Frequency Wireless Mobile Networks," in *Proc. IEEE GLOBECOM Conference*, Singapore, 2017, pp. 1-7.
- [25] M. Comiter, and H. T. Kung, "Localization Convolutional Neural Networks Using Angle of Arrival Images," in *Proc. IEEE Global Communications Conference*, Abu Dhabi, Dec. 2018, pp. 1-7.
- [26] A. Khan, S. Wang and Z. Zhu, "Angle-of-Arrival Estimation Using an Adaptive Machine Learning Framework," *IEEE Communications Letters*, vol. 23, no. 2, pp. 294-297, Feb. 2019.
- [27] X. Wang, X. Wang, and S. Mao, "CiFi: Deep convolutional neural networks for indoor localization with 5 GHz Wi-Fi," *IEEE International Conference on Communications (ICC)*, pp. 1-6, May 2017.
- [28] X. Wang, X. Wang and S. Mao, "Deep Convolutional Neural Networks for Indoor Localization with CSI Images," *IEEE Transactions on Network Science and Engineering*, vol. 7, no. 1, pp. 316-327, Mar. 2020.
- [29] Z. HajiAkhondi-Meybodi, M. S. Beni, A. Mohammadi, and K. N. Plataniotis, "Bluetooth Low Energy-based Angle of Arrival Estimation in Presence of Rayleigh Fading," *IEEE International Conference on Systems, Man, and Cybernetics*, 2020.
- [30] H. Zhang, J. Hu, H. Zhang, B. Di, K. Bian, Z. Han, and L. Song, "MetaRadar: Indoor Localization by Reconfigurable Metamaterials," *IEEE Transactions on Mobile Computing*, Dec. 2020.